X-Ray Analyses of Complexes Formed between Surfactants and Aromatic Compounds. I. A Common Structural Pattern of the Complexes

Keiju Sawada, Tatsuo Kitamura, Yuji Ohashi,* Nahoko Iimura,† and Hirotaka Hirata†

Department of Chemistry, Tokyo Institute of Technology, 2-12-1 O-okayama, Meguro-ku, Tokyo 152

†Department of Physical Chemistry, Niigata College of Pharmacy, 2-13-5 Kamishin'eicho, Niigata 950-21

(Received April 27, 1998)

The cationic surfactants such as hexadecyl-, tetradecyl-, dodecyl-, and decyltrimethylammonium bromides form complexes with a variety of aromatic compounds in aqueous solutions. Well-defined crystals were obtained if the aromatic compounds had hydrogen donor moieties. The structures of ten kinds of the complex crystals were analyzed by X-rays. All the crystal structures had a common pattern of complex formation, in which the aromatic compounds are sandwiched by the two alkyl chains of the surfactant molecules. There are two modes of stacking when the complexes with the common pattern are piled up to form the crystalline lattice. The common pattern of complex formation is responsible for the high viscoelasticity of the aqueous solutions containing cationic surfactants and aromatic compounds.

An aqueous solution containing a surfactant forms micelles at concentrations above a critical value, which is called the critical micelle concentration (cmc). The value of cmc is approximately 10^{-4}—10^{-2} M (1 M = 1 mol dm^{-3}) in the case of cationic or anionic surfactants, and below 10^{-4} M in the case of nonionic surfactants.[1] If some aromatic compounds are dissolved in the aqueous solution containing a surfactant, the micelles are formed containing the aromatic compounds at concentrations less than the cmc.[2,3] Several works have proposed structures and properties for the micelles. By ^{1}H NMR chemical shifts it was proposed that the benzene molecule should be placed near the surface of the micelle of hexadecyltrimethylammonium bromide in aqueous solution.[4] The same model was proposed from pulse radiolysis.[5] However, the opposite model, that the benzene molecules were placed at the center of micelles, was proposed from the ultraviolet absorption spectrum.[6] The proposed current model of micellar aggregates in aqueous solution affords insufficient explanations for the available data and often gives rise to contradiction.[7,8] Micelles with platelet or rod-like shapes were obtained in supersaturated aqueous solution containing a surfactant and an aromatic compound. Particularly, chiral surfactants are known to produce enantiomeric precipitation, while most of the others give symmetrical micelles.[9—11]

Electron microscopy showed that gigantic rod-like micelles were formed in viscoelastic solutions in the presence of several aromatic compounds.[12—14] In these viscoelastic solutions, single crystals were found to exist mixed with gigantic micelles.[15] From the aqueous solution composed of hexadecyltrimethylammonium bromide and *o*-iodophenol, single crystals suitable for X-ray work were obtained.[16]

We tried the single crystal formation with different combinations of surfactants and aromatic compounds. A variety of complex crystals have been obtained. Table 1 lists the complex crystals between four surfactant molecules such as hexadecyl-, tetradecyl-, dodecyl-, and decyltrimethylammonium bromide (hereafter abbreviated to CTAB, MTAB, LTAB, and DTAB, respectively) and various aromatic compounds. Moreover, several complexes between cationic surfactants molecules with odd alkyl chains or anionic surfactant and aromatic compounds, such as (tridecyl)trimethylammonium bromide and biphenyl, pentadecyltrimethylammonium bromide and biphenyl, and sodium dodecyl sulfate and ethyl phenyl ether, were obtained. Most of the crystal structures suitable for X-ray works have been analyzed by X-rays. A common structural pattern is observed in the analyzed structures. This paper reports ten typical kinds of complex crystal structures in Table 1 and proposes a model for the micelle formation.

Experimental

Preparation of Complex Crystals. The complex crystals were prepared by mixing aqueous solutions of the surfactants and aromatic compounds in a 1 : 1—1 : 2 molar ratio. The precipitate was purified by repeated crystallizations in aqueous solutions. All the obtained crystals were colorless and plate-like. To detach the sheets of plate-like crystals, the crystals were washed several times by cold water.

Crystal Structure Analyses. The crystal data and experimental details are summarized in Table 2. The ten crystals (I to X) were mounted on four-circle diffractometers (Rigaku-AFC4, Rigaku-AFC5R, and Rigaku-AFC7S) using Cu $K\alpha$ or Mo $K\alpha$ radiation monochromated by graphite. The crystals of II, III, IV, VI, and VII were sealed in glass capillaries since they are easily decomposed in open air. The temperature was cooled down to 238 K with the cold nitrogen-gas-flow method for the crystals of I, VI, VII, VIII, and

Table 1. Suitable for X-Ray Works, the List of the Complex Crystals between Cationic Surfactants and Aromatic Compounds

	C	M	L	D
o-Iodophenol	◎	◎	◎	◎
m-Iodophenol	○	–	○	○
p-Iodophenol	○	–	○	○
p-Cresol	◎	–	–	–
m-Cyanophenol	◎	–	○	○
o-Hydroxybenzoic acid	○	○	○	○
m-Hydroxybenzoic acid	○	◎	○	○
p-Hydroxybenzoic acid	◎	–	×	◎
o-Toluic acid	×	–	○	○
m-Toluic acid	×	–	○	○
p-Toluic acid	×	–	×	○
o-Phtalic acid	×	–	–	–
m-Phtalic acid	×	–	–	–
p-Phtalic acid	×	–	–	–
Hydroquione	◎	–	○	○
1,4-Dimethoxybenzene	×	–	×	–
p-Benzoquinone	–	–	×	–
1,4-Cyclohexanediol	×	–	×	×
Naphthalene	×	–	–	○
1-Naphthol	○	–	○	○
2-Naphthol	○	–	○	○
Indole	◎	–	○	○
7-Hydroxycoumarin	×	×	×	○
Coumarin	×	–	×	○

	C	M	L	D
2-Aminopyridine	○	○	○	○
3-Aminopyridine	○	–	○	○
4-Aminopyridine	×	–	○	○
2-Hydroxypyridine	×	–	○	○
3-Hydroxypyridine	×	–	×	○
4-Hydroxypyridine	×	–	×	○
3-Cyanopyridine	×	×	×	×
4-Cyanopyridine	×	–	×	×
4-Dimethylaminopyridine	×	–	–	○
2-Phenylpyridine	◎	○	○	○
3-Phenylpyridine	○	○	○	○
4-Phenylpyridine	◎	○	○	○
2,2′-Bipyridine	○	○	○	○
2,4-Bipyridine	○	○	○	○
4,4′-Bipyridine	○	○	○	○
Anthracene	×	–	○	○
Acridine	◎	–	○	○
Phenanthrene	○	○	○	○
Benzo[*h*]quinoline	×	–	○	○
Benzo[*f*]quinoline	×	–	○	○
1,1′-biphenyl-4-ol	◎	◎	◎	○
Bibenzyl	×	–	×	×
Biphenyl	◎	◎	◎	◎
Carbazole	◎	○	○	○
Dibenzofuran	◎	○	○	○
Diphenylamine	◎	○	○	○

The symbols of ◎, ○, ×, and – represent the single crystals, the only powdered crystals, no complex crystals, and not tried. The symbols of C, M, L, and D are surfactants of CTAB, MTAB, LTAB, and DTAB, respectively. The list omit the other surfactants, anionic surfactants or surfactants with odd alkyl part, and some of aromatic compounds.

IX. The unit-cell parameters for each crystal were refined by least-squares fitting using the angular settings of 15 reflections in the 2θ ranges of $40° < 2\theta < 50°$ for Cu $K\alpha$ radiation and $20° < 2\theta < 25°$ for Mo $K\alpha$ radiation.

The structures were solved by the direct method with the program SHELXS86[17] and were refined by full-matrix least-squares with the program SHELXL97.[18] Since it was too difficult to refine all the non-hydrogen atoms with anisotropic temperature factors, some of the non-hydrogen atoms were refined with the isotropic temperature factors. The C–C bonds and C–C–C angles in aromatic rings were constrained to 1.39 Å and 120°. The C≡N triple and C–C bonds in *m*-cyanophenol of the crystal II were restrained to 1.138(1) and 1.437(1) Å, respectively. The C–CH_3 and C–O bonds in *p*-cresol of the crystal III were restrained to 1.506(11) and 1.362(15) Å, respectively. Three N–CH_3 bonds in CTAB of the crystal IV were restrained to 1.47(1) Å. The positions of all hydrogen atoms were calculated and fixed. The weighting scheme applied to all the crystals is $1/[\sigma^2(F_0^2)+(aP)^2+bP]$ where $P = (F_0^2+2F_c^2)/3$. The final R values of III, IV, and VI are somewhat high (>0.10). This is probably due to the disordered structures of alkyl chains and/or aromatic rings. Moreover, the thickness of the plate-like crystals of III, IV, and VII are too thin. Although the Mo $K\alpha$ radiation should be used for VI, VII, VIII, and IX since they have iodine atoms, the Cu $K\alpha$ radiation was used because the c axis lengths of these crystals are too long. The atomic scattering factors including the dispersion terms were taken from International Tables for Crystallography.[19] Lists of final atomic parameters, bond distances and angles, and structure factors for the ten crystals have been deposited as Document No. 71048 at the Office of the Editor of Bull. Chem. Soc. Jpn.

Results

Crystal Structure of I (CTAB+*p*-Hydroxybenzoic Acid). The crystal structure viewed along the b and c axes are shown in Fig. 1. There are three hexadecyltrimethylammonium (CTA) cations and bromide anions, two *p*-hydroxybenzoic acid (*p*-HBA) molecules and one solvent water in the asymmetric unit. The molecular structures with the atomic numberings are shown in Fig. 2. The bond distances and angles are not significantly different among the corresponding ones of the crystallographically independent molecules. The CTA moieties with all-*trans* conformation run antiparallel alternately along the a axis. The *p*-HBA molecule is sandwiched by the alkyl chains of CTA and situated between the alkyl group and the bromide anion. The carboxy groups of the A and B *p*-HBA molecules form a dimer through the double O–H···O hydrogen bonds. The hydroxy groups of A and B *p*-HBA also make hydrogen bonds and the hydroxy group of A also makes a hydrogen bond with the solvent water molecule which is hydrogen-bonded with the bromide anions. The hydrogen bond distances are listed in Table 3. The bromide anions and trimethylammonium moieties form the respective ribbons along the c axis. The hydrophobic ribbon composed of the alkyl group of CTA and *p*-HBA extends along the c axis. The hydrophobic ribbon composed of the bromide anion and trimethylammonium cation and the hydrophobic ribbon are packed alternately, making a 'planar

Table 2. Crystal Data and Experimental Details for Ten Crystal Forms

	I	II	III	IV	V	VI	VII	VIII	IX	X
	CTAB/ *p*-Hydroxybenzoic acid	CTAB/ *m*-Cyanophenol	CTAB/ *p*-Cresol	CTAB/ Acridine	CTAB/ Hydroquinone	CTAB/ *o*-Iodophenol	MTAB/ *o*-Iodophenol	LTAB/ *o*-Iodophenol	DTAB/ *o*-Iodophenol	DTAB/ *p*-Hydroxybenzoic acid
Chemical formula	$3C_{19}H_{42}NBr/2C_7H_6O_3/H_2O$	$C_{19}H_{42}NBr/0.5C_7H_5ON$	$C_{19}H_{42}NBr/C_7H_8O$	$C_{19}H_{42}NBr/0.5C_{13}H_9N$	$C_{19}H_{42}NBr/C_6H_6O_2/2H_2O$	$C_{19}H_{42}NBr/C_6H_5OI$	$C_{17}H_{38}NBr/C_6H_5OI$	$C_{15}H_{34}NBr/C_6H_5OI$	$C_{13}H_{30}NBr/C_6H_5OI$	$C_{13}H_{30}NBr/C_7H_6O_3/H_2O$
Formula weight	1387.59	424.01	472.58	454.05	510.59	584.45	556.39	528.34	500.29	436.42
Crystal system	Monoclinic	Monoclinic	Monoclinic	Monoclinic	Monoclinic	Orthorhombic	Orthorhombic	Monoclinic	Monoclinic	Monoclinic
Space group	$P2_1$	$P2_1$	$P2_1$	$P2_1$	$P2_1/n$	$Pna2_1$	$Pca2_1$	$P2_1/n$	$P2_1/n$	$C2$
Z	2 (3 : 2 : w1)	2 (1 : 0.5)	2 (1 : 1)	2 (1 : 0.5)	4 (1 : 1 : w2)	8 (1 : 1)	8 (1 : 1)	8 (1 : 1)	4 (1 : 1)	4 (1 : 1 : w1)
a/Å	33.972(2)	33.767(3)	32.303(3)	32.066(2)	8.3546(9)	17.231(2)	17.288(3)	8.269(7)	8.302(3)	30.003(2)
b/Å	7.3057(19)	7.4700(10)	7.4737(5)	7.4014(7)	52.182(2)	8.5132(6)	8.292(7)	33.130(6)	30.349(3)	7.466(4)
c/Å	16.283(2)	5.5750(10)	5.5743(5)	5.5898(4)	7.1699(8)	39.167(4)	37.327(13)	9.073(6)	9.020(2)	10.857(4)
β/°	94.208(8)	107.076(7)	92.187(11)	91.602(8)	109.210(8)	—	—	94.54(5)	95.52(2)	101.957(12)
V/Å^3	4030.4(12)	1344.2(3)	1344.79(19)	1326.13(18)	2951.7(5)	5745.3(10)	5351(5)	2478(3)	2262.0(9)	2379.2(15)
D_x/Mg m^{-3}	1.143	1.048	1.167	1.137	1.149	1.351	1.381	1.416	1.469	1.218
Diffractometer	AFC5R	AFC4	AFC4	AFC4	AFC4	AFC4	AFC4	AFC5R	AFC5R	AFC7S
Radiation	Cu $K\alpha$	Cu $K\alpha$	Cu $K\alpha$	Cu $K\alpha$	Cu $K\alpha$	Cu $K\alpha$	Cu $K\alpha$	Cu $K\alpha$	Cu $K\alpha$	Mo $K\alpha$
λ/Å	1.54184	1.54184	1.54184	1.54184	1.54184	1.54184	1.54184	1.54184	1.54184	0.71703
μ/mm^{-1}	2.209	2.122	2.178	2.169	2.096	10.479	11.224	12.091	13.211	1.749
T_{max}	0.6081	0.6762	0.8989	0.8993	0.6792	0.2284	0.4671	0.1959	0.0766	0.5413
T_{min}	0.4364	0.5685	0.6120	0.5173	0.4877	0.0774	0.0811	0.0856	0.0581	0.4751
$F(000)$	1496	458	512	490	1104	2400	2272	1072	1008	928
Color of crystal	Colorless	Colorless	Colorless	Colorless	Colorless	Colorless	Colorless	Colorless	Colorless	Colorless
Shape of crystal	Plate	Plate	Plate	Plate	Plate	Plate	Plate	Plate	Plate	Plate
Crystal dimensions/mm^3	0.45 × 0.35 × 0.25	0.30 × 0.25 × 0.20	0.25 × 0.25 × 0.05	0.35 × 0.30 × 0.05	0.40 × 0.40 × 0.20	0.50 × 0.35 × 0.20	0.45 × 0.25 × 0.08	0.40 × 0.30 × 0.20	0.50 × 0.40 × 0.40	0.50 × 0.40 × 0.40
T/K	238	296	296	296	296	238	238	238	238	296
Maximum 2θ/°	125	125	125	125	125	125	125	125	125	55
Range of h	0 → 39	−38 → 37	−37 → 36	−36 → 36	−9 → 9	−19 → 0	−19 → 0	−9 → 9	0 → 9	−38 → 38
Range of k	0 → 8	0 → 8	−8 → 0	−8 → 0	0 → 60	0 → 9	0 → 9	0 → 38	0 → 34	0 → 9
Range of l	−18 → 18	0 → 6	0 → 7	0 → 6	0 → 8	0 → 45	0 → 42	0 → 10	−10 → 10	0 → 12
Scan technique	$2\theta/\omega$-scan	$2\theta/\omega$-scan	$2\theta/\omega$-scan	$2\theta/\omega$-scan	ω-scan	$2\theta/\omega$-scan	ω-scan	$2\theta/\omega$-scan	$2\theta/\omega$-scan	ω-scan
standards number	3	3	3	3	3	3	3	3	3	3
standards interval (count)	100	50	50	50	50	50	50	50	50	100
Absorption correction	Psi-scan	None	None	None	None	None	None	Psi-scan	Psi-scan	Psi-scan
No. of measured reflections	7088	2398	2781	2683	5167	5368	4961	4327	3981	6307
No. of independent reflections	6959	2348	2349	2324	4817	5179	4806	4056	3708	5384
No. of used reflections	6955	2344	2345	2320	4728	4620	4132	3892	3565	2689
No. of parameters	733	205	119	126	269	219	202	227	198	223
Weighting parameter										
a	0.0526	0.1871	0.1989	0.2881	0.0634	0.2000	0.1369	0.1220	0.0957	0.0488
b	0.2641	0	0	0	0.6568	0	0	0	2.112	0.2231
R ($I > 2\sigma$)	0.0300	0.0979	0.1080	0.1348	0.0452	0.1269	0.0959	0.0726	0.0466	0.0409
wR (F^2)	0.0895	0.2613	0.2962	0.3847	0.1117	0.3028	0.2175	0.1934	0.1253	0.0908
Goodness-of-fit on F^2	1.088	1.034	1.016	1.114	1.077	1.094	0.933	1.057	1.052	0.970
$\delta\rho$/e Å^{-3}	+0.367,−0.306	+1.190,−0.612	+1.254,−0.690	+1.514,−1.304	+0.602,−0.518	+3.943,−2.067	+0.975,−1.585	+0.977,−1.126	+1.162,−1.612	+0.180,−0.185

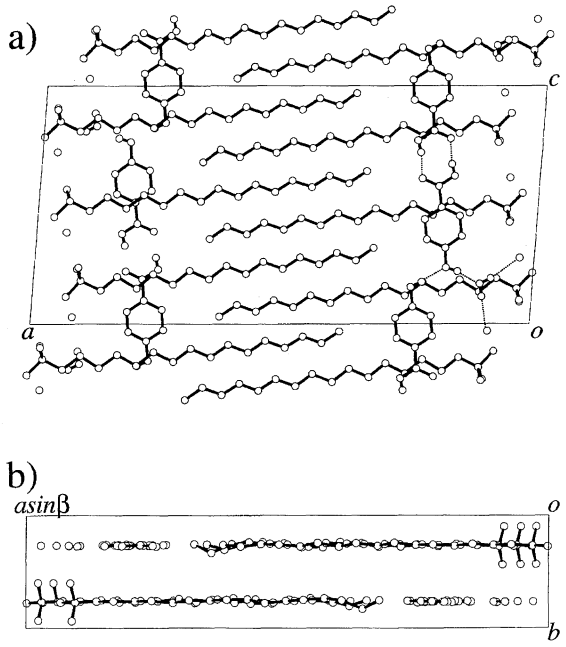

Fig. 1. Crystal structures of I viewed along the *b*; a) and *c*; b) axes. Hydrogen bond network is shown with dashed lines, the distances of which are summarized in Table 3.

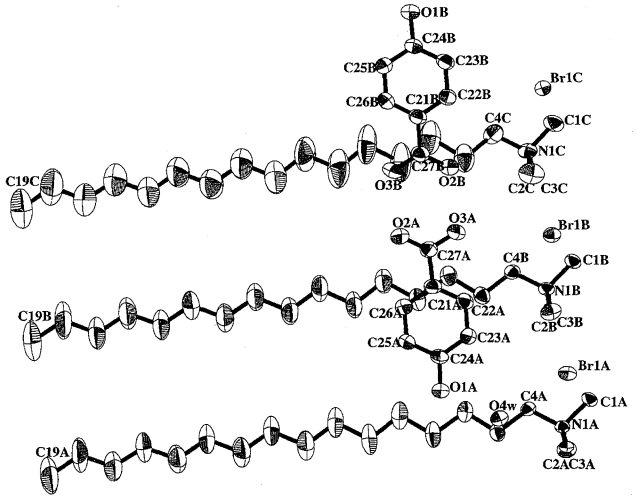

Fig. 2. ORTEP drawing of the molecular structure I showing 50% thermal ellipsoids and the numbering of atoms. The numbers from C5A to C18A, from C5B to C18B and from C5C to C18C of CTAB are omitted.

Table 3. Hydrogen Bond Distances of the Crystal I

Br1A–O4W	3.2160(15)
O1A–O4W	2.562(2)
O1A–O1B$^{\#1}$	2.735(2)
O2A–O3B	2.609(2)
O3A–O2B	2.572(2)
O4W–Br1C$^{\#1}$	3.2659(14)

The symbols of #1 indicates the equivalent atoms of $(x, y, z-1)$.

sheet' parallel to the *ac* plane.

Crystal Structure of II (CTAB+*m*-Cyanophenol). The crystal structure viewed along the *b* and *a* axes is shown in Fig. 3. Since the occupancy factor of the *m*-cyanophenol (*m*-CP) molecule is 0.5, there is one *m*-CP, on average, in the two unit cells along the *c* axis. This means that there are no unusually short contacts between the *m*-CP molecules. The molecular structure with the atomic numbering is shown in Fig. 4. The bond distances and angles are substantially the same as the corresponding ones of the related compounds. The CTA cations with all-*trans* conformation run antiparallel alternately along the *a* axis. The *m*-CP molecule is sandwiched by the alkyl chains of CTAs along the *b* axis and is situated between CTA cation and the bromide anion along the *a* axis. The OH group of *m*-CP is hydrogen-bonded to the bromide anion (O–H···Br 3.08(3) Å). The bromide anions and trimethylammonium moieties form the respective ribbons along the *c* axis. The hydrophobic ribbon composed of the alkyl group of CTA and *m*-CP extends along the *c* axis. The hydrophilic ribbon composed of the bromide anion and trimethylammonium cation and the hydrophobic ribbon are packed alternately, making a "planar sheet" parallel to the *ac* plane. These features are substantially the same as those of the crystal I.

Crystal Structure of III (CTAB+*p*-Cresol). The crystal structure is isomorphous to that of the crystal of II, as shown in Fig. 5. The *p*-cresol molecule takes two disordered structures, the occupancy factors of which are 0.65 and 0.35. To avoid short contacts between the *p*-cresol molecules, the conformations of the neighboring *p*-cresol molecules along the *c* axis should be different from each other. The molecular structure with the atomic numbering is shown in Fig. 6. The bond distances and angles are not significantly different from the corresponding ones of the related compounds. The OH group of *p*-cresol is hydrogen-bonded to the bromide anion (O–H···Br 2.99(2) and 3.44(4) Å for the two disordered OH

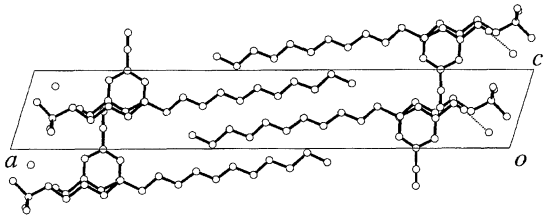

Fig. 3. Crystal structure of II viewed along the *b* axis. Hydrogen bonds are show with dashed lines.

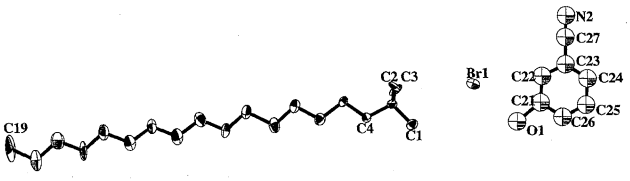

Fig. 4. ORTEP drawing of the molecular structure II showing 30% thermal ellipsoids and the numbering of atoms. The numbers from C5 to C18 of CTAB are omitted. The atoms of *m*-cyanophenol molecule were refined isotropically.

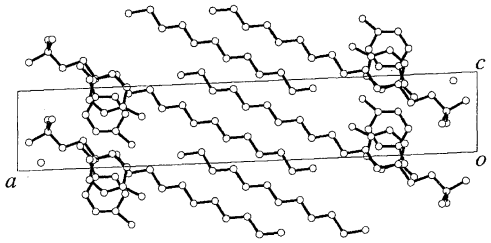

Fig. 5. Crystal structure of III viewed along the *b* axis.

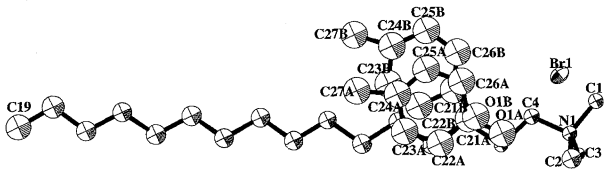

Fig. 6. ORTEP drawing of the molecular structure III showing 30% thermal ellipsoids and the numbering of atoms. The numbers from C5 to C18 of CTAB are omitted. The atoms of CTA cation and *p*-cresol molecules were refined isotropically.

groups). The hydrophilic ribbon composed of the bromide anion and trimethylammonium cation and the hydrophobic ribbon composed of the alkyl group and *p*-cresol are packed alternately, making a "planar sheet" parallel to the *ac* plane. The structural characteristics are substantially the same as those of the crystals I and II.

Crystal Structure of IV (CTAB + Acridine). The crystal structure is isomorphous to the crystals of II and III, as shown in Fig. 7. Since the occupancy factor of the acridine molecule is 0.5, there is one acridine molecule, on average, in the two unit cells along the *c* axis. The molecular structure with the atomic numbering is shown in Fig. 8. The bond distances and angles are not significantly different from the corresponding ones of the related compounds. Although there is no hydrogen bond between acridine and the bromide anion, the intermolecular distance between the H atoms of the acridine ring and bromide anion is slightly shorter than the van der Waals contact; this means weak hydrogen bonds. The hydrophilic ribbon composed of the bromide anion and trimethylammonium cation and the hydrophobic ribbon composed of the alkyl group and acridine are packed alternately, making a "planar sheet" parallel to the *ac* plane. The structural characteristics are similar to those of the crystals, I, II, and III.

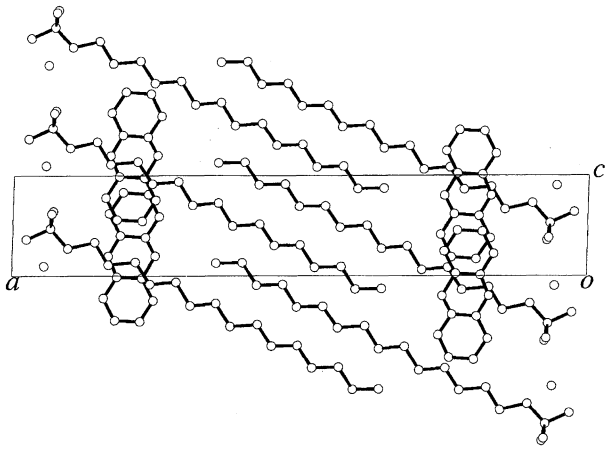

Fig. 7. Crystal structure of IV viewed along the *b* axis.

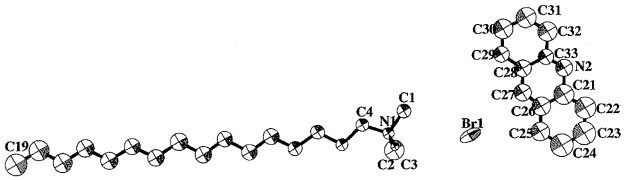

Fig. 8. ORTEP drawing of the molecular structure IV showing 50% thermal ellipsoids and the numbering of atoms. The numbers from C5 to C18 of CTAB are omitted. The atoms of CTA cation and acridine molecule were refined isotropically.

Crystal Structure of V (CTAB + Hydroquinone). The crystal structures viewed along the *b* and *a* axes are shown in Fig. 9. There are one CTA cation, one bromide anion, one hydroquinone, and two water molecules (A and B) in an asymmetric unit. The molecular structure with the atomic numbering is shown in Fig. 10. One OH group of the hydroquinone molecule is hydrogen-bonded with another OH group of the hydroquinone molecule along the *c* axis, (O2–H···O1, 2.731(3) Å). The latter OH group is hydrogen-bonded with the water molecule O3w (O1–H···O3w, 2.623(3) Å), which is also hydrogen-bonded with the bromide anion and another water molecule O4w (O3w–H···Br, 3.261(2) Å and O3w–H···O4w, 2.731(4) Å, respectively). The water molecule O4w is hydrogen-bonded with the bromide anions related to the glide plane (O4w–H···Br, 3.286(2) and 3.295(2) Å). These hydrogen bonds connect the hydrophilic parts as a layer parallel to the *ac* plane. As shown in the crystal structures I to IV, the CTA cation, hydroquinone, and bromide anion are packed as a sheet along the *a* axis. However, the sheet is bent at the hydrophilic layer. This makes a "pleated sheet" parallel to the *bc* plane.

Crystal Structure of VI (CTAB+*o*-Iodophenol). The crystal structures viewed along the *b* and *a* axes are shown in Fig. 11. There are two CTA cations and bromide anions, and two *o*-iodophenol molecules in an asymmetric unit. The molecular structure with the atomic numbering is shown in Fig. 12. The OH groups of the *o*-iodophenol molecule are hydrogen-bonded with the bromide anions (O–H···Br 3.184(14) and 3.326(17) Å, respectively). The bromide anions and trimethylammonium moieties form the respective ribbons along the *b* axis. The hydrophobic ribbon composed of the alkyl group of CTA and *o*-iodophenol extends along the *b* axis. The hydrophilic ribbon composed of the bromide anion and trimethylammonium cation and the hydrophobic ribbon are packed alternately, making a "pleated sheet" parallel to the *bc* plane. The pleated sheets are piled up along the *a* axis to make a crystal. These features are substantially the same as those of the crystal V.

Crystal Structure of VII (MTAB+*o*-Iodophenol). The crystal structure viewed along the *b* axis is shown in Fig. 13. There are two MTA cations and bromide anions, and two *o*-

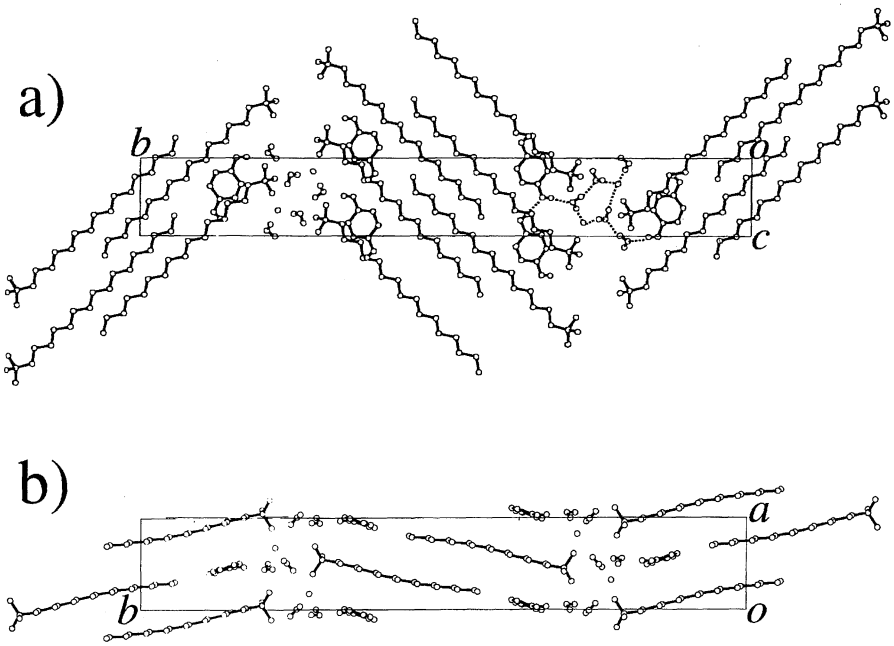

Fig. 9. Crystal structures of V viewed along the *a*; a) and *c*; b) axes. Hydrogen bond network is shown with dashed lines.

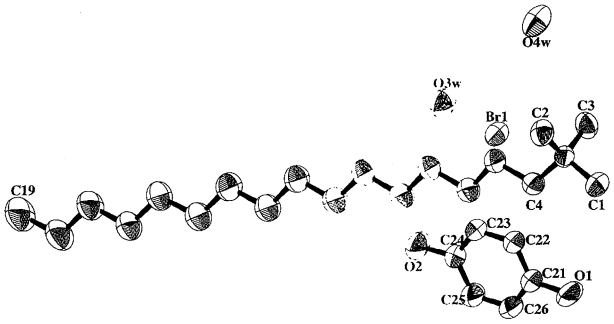

Fig. 10. ORTEP drawing of the molecular structure V showing 50% thermal ellipsoids and the numbering of atoms. The numbers from C5 to C18 of CTAB are omitted.

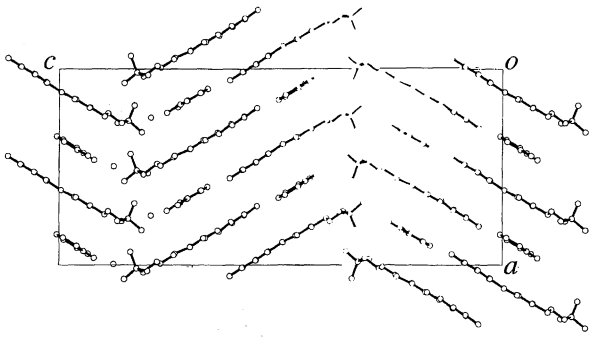

Fig. 11. Crystal structure of VI viewed along the *b* axis.

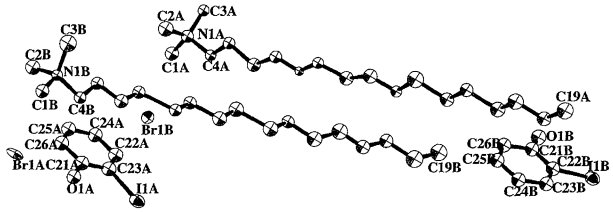

Fig. 12. ORTEP drawing of the molecular structure VI showing 50% thermal ellipsoids and the numbering of atoms. The numbers from C5A to C18A and from C5B to C18B of CTAB are omitted. The C and N atoms were refined isotropically.

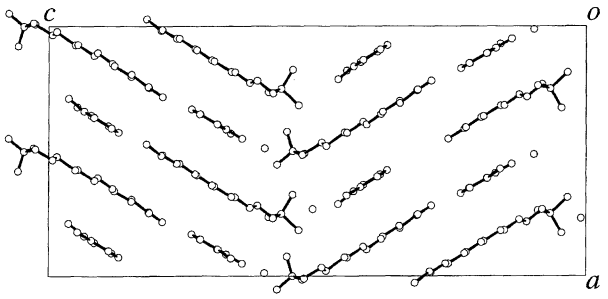

Fig. 13. Crystal structure of VII viewed along the *b* axis.

iodophenol molecules in an asymmetric unit. The molecular structure with the atomic numbering is shown in Fig. 14. The OH groups of the *o*-iodophenol molecule are hydrogen bonded with the bromide anions (O–H···Br 3.19(2) and 3.16(2) Å, respectively). The packing mode of the MTA molecules and the bromide anions is nearly the same as that of the CTAB+*o*-iodophenol crystal, VI. The "pleated sheet" is parallel to the *bc* plane and the sheets are stacked along the *a* axis.

Crystal Structure of VIII (LTAB+*o*-Iodophenol). The crystal structure viewed along the *a* axis is shown in Fig. 15. There are one LTA cation and bromide anion, and one *o*-iodophenol molecule in an asymmetric unit. The molecular structure with the atomic numbering is shown in Fig. 16. The OH group of the *o*-iodophenol molecule is hydrogen-bonded with the bromide anion (O–H···Br 3.176(8) Å). The packing mode of the LTA cations and the bromide anions are nearly the same as those of VI and VII. The "pleated sheet" is parallel to the *ab* plane and the sheets are stacked along

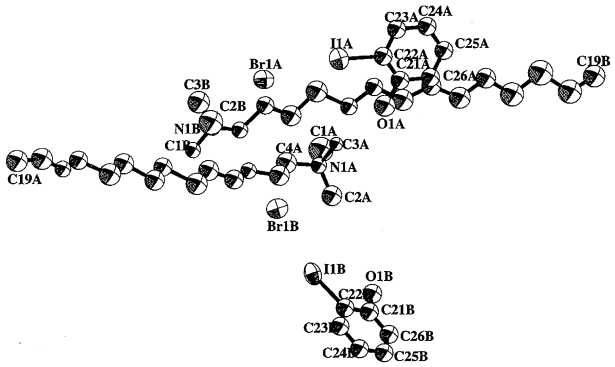

Fig. 14. ORTEP drawing of the molecular structure VII showing 50% thermal ellipsoids and the numbering of atoms. The numbers from C5A to C16A and from C5B to C16B of MTAB are omitted. The C and N atoms were refined isotropically.

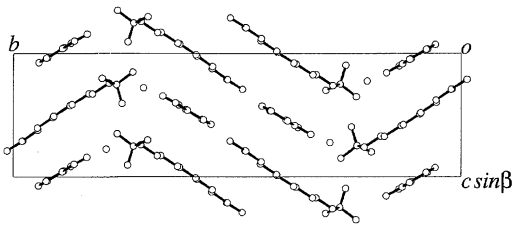

Fig. 15. Crystal structure of VIII viewed along the *a* axis.

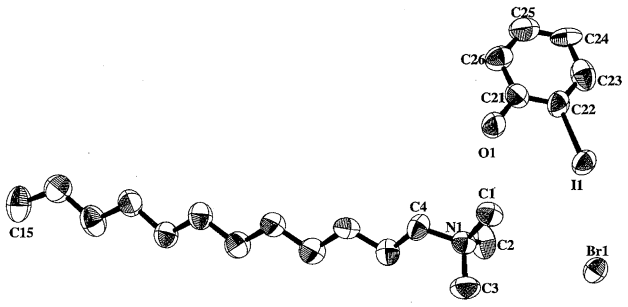

Fig. 16. ORTEP drawing of the molecular structure VIII showing 50% thermal ellipsoids and the numbering of atoms. The numbers from C5 to C14 of LTAB are omitted.

the *c* axis.

Another form, which is isomorphous to VI and VII, was crystallized under the same conditions. The cell dimensions are a = 17.239(4), b = 8.286(1), c = 35.308(16) Å, and V = 5043(3) Å^3, $Pca2_1$ and Z = 8. The three-dimensional intensity data were collected and the structure was identified. Although the converged R value was 0.16 because of the poor crystallinity, the structure obtained is very similar to that of VII, except that the alkyl chain of the surfactant molecule is shorter than that of VII.

Crystal Structure of IX (DTAB+*o*-Iodophenol). The crystal structure viewed along the *a* axis is shown in Fig. 17. There are one DTA and bromide anion, and one *o*-iodophenol molecule in an asymmetric unit. The molecular structure with the atomic numbering is shown in Fig. 18. The OH group of the *o*-iodophenol molecule is hydrogen-bonded with the bromide anion (O–H···Br 3.175(5) Å). The structure is

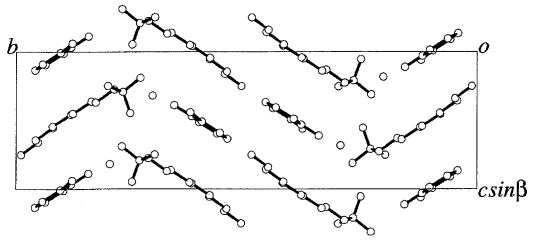

Fig. 17. Crystal structure of IX viewed along the *a* axis.

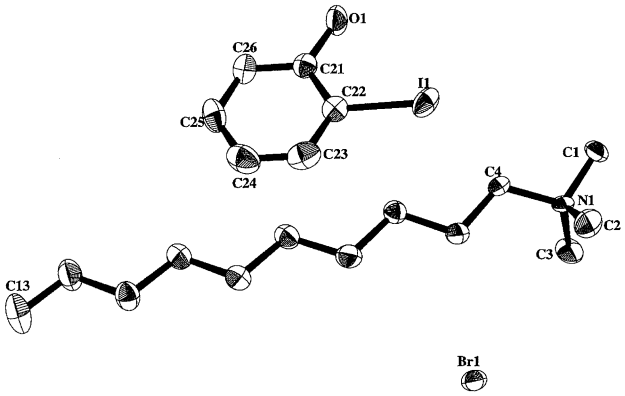

Fig. 18. ORTEP drawing of the molecular structure IX showing 50% thermal ellipsoids and the numbering. The numbers from C5 to C12 of DTAB are omitted.

isomorphous to that of LTAB+*o*-iodophenol crystal, VIII, and very similar to VI and VII. The "pleated sheet" is parallel to the *ab* plane and the sheets are stacked along the *c* axis.

Crystal Structure of X (DTAB+*p*-Hydroxybenzoic Acid). The crystal structures viewed along the *b* and *c* axes are shown in Fig. 19. There are one DTA cation and bromide anion, one *p*-hydroxybenzoic acid (*p*-HBA) molecule, and one solvent water in an asymmetric unit. Although the structure has pseudo-mirror symmetry, they were not refined with mirror symmetry because the R value became worse and the refined molecular structures were somewhat distorted. The molecular structures with the atomic numberings are shown

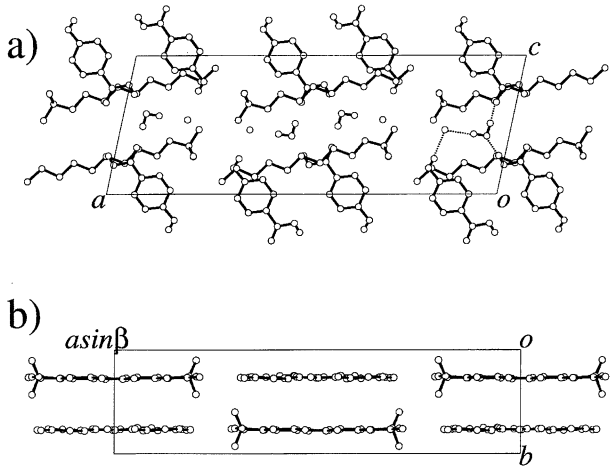

Fig. 19. Crystal structures of X viewed along the *b*; a) and *c*; b) axes. Hydrogen bond network is shown with dashed lines, the distances of which are summarized in Table 4.

in Fig. 20. The bond distances and angles are not significantly different from the corresponding ones of the related molecules. The DTA molecules with all-*trans* conformation run antiparallel alternately along the [1 0 $\bar{1}$] direction. The carboxy groups of *p*-HBA form a dimer through the double O–H···Ow–H···O hydrogen bonds. The hydroxy group of *p*-HBA makes a hydrogen bond with the bromide anion, which also makes a hydrogen bond with the solvent water molecule. The *p*-HBA molecule is sandwiched by the alkyl chains of DTA. The hydrogen bond distances are listed in Table 4. The bromide anions and trimethylammonium moieties form the respective ribbons along the *c* axis. The hydrophobic ribbon composed of the alkyl group of DTA extends along the *c* axis. Since the direction of the dimer structure of *p*-HBA is not parallel to the *c* axis, the antiparallel contacts of the alkyl chains of DTA are not formed. This causes the layer structure to be parallel to the *bc* plane. The inner part of the layer is composed of the hydrophobic one while both outsides of the layer are made of hydrophilic ones. Moreover, a "planar sheet" is formed parallel to the *ac* plane.

Discussion

Common Pattern of the Complexes. The complex formations between the cationic surfactants and the aromatic compounds described above have common features as follows;

(1) The trimethylammonium moieties of the surfactant molecules and the bromide anions form a hydrophilic layer.

(2) The alkyl chains of the surfactant molecules with all-*trans* conformation grow from the above hydrophilic layer.

(3) The aromatic molecule is sandwiched by the alkyl groups of the two surfactant molecules and makes hydrogen bond(s) with the bromide anion directly or through the solvent water molecule, except for the acridine complex.

(4) The above aggregation forms a layer structure, which is schematically shown in Fig. 21. One side of the layer is the hydrophilic one composed of the trimethylammonium cation and the bromide anion. In some cases the solvent water molecules are included. Another side of the layer is the hydrophobic one, composed of the alkyl group of the surfactant molecule and the aromatic molecule if the alkyl chain is short.

(5) The alkyl chains of the two layers are engaged as to make a common packing pattern of the layer structure in which the antiparallel stacking of the alkyl chains is formed, as shown in the left-side drawings of Fig. 22.

(6) If the alkyl chain of the surfactant is long enough, the antiparallel alkyl chains have close contacts between them as shown in CTAB complexes. As the alkyl chain becomes shorter, the interaction between the alkyl group and the aromatic compound prevents such a close contact between the alkyl groups.

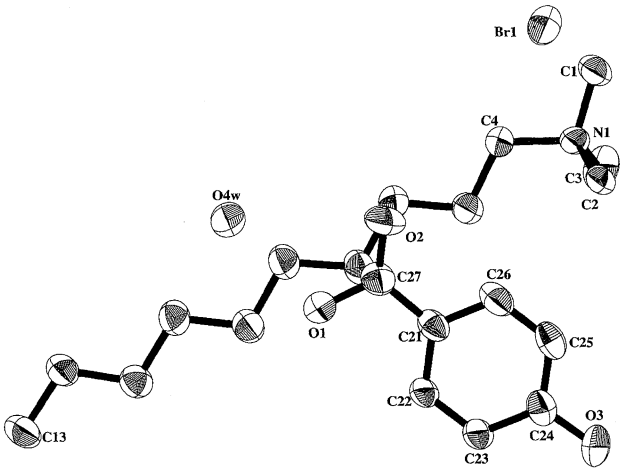

Fig. 20. Ortep drawing of the molecular structure X showing 30% thermal ellipsoids and the numbering. The numberings from C5 to C12 of DTAB are omitted.

Table 4. Hydrogen Bond Distances of the Crystal X

O4W–O1	2.583(5)
Br1–O3$^{\#1}$	3.170(4)
Br1–O4W$^{\#2}$	3.233(4)
O2–O4W$^{\#2}$	2.690(5)

The symbols of #1 and #2 indicate the equivalent atoms of (x, y, $z+1$) and ($-x+2$, y, $-z+1$), respectively.

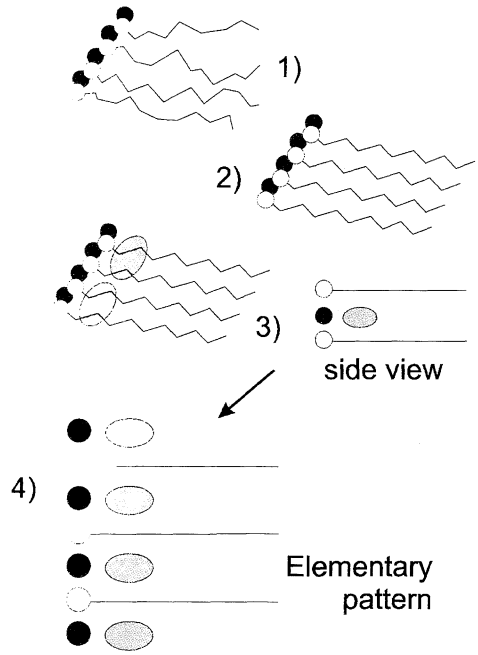

Fig. 21. Schematic drawings of the complex formation between the cationic surfactants and the aromatic compounds. The white and gray circles indicate the trimethylammonium moiety of the surfactant and the bromide anion, respectively. The alkyl group of the surfactant and the aromatic compound are shown with a solid lines and the gray ellipsoid, respectively. When the surfactant is solved in a solution, the ionic interaction makes the hydrophilic layer as indicated white circles. From the layer the alkyl chains are arranged irregularly, 1), or regularly, 2). If the aromatic molecules make a complex with the alkyl chains, the regularly ordered pattern, 3) or 4) is formed, which is called as an elementary pattern.

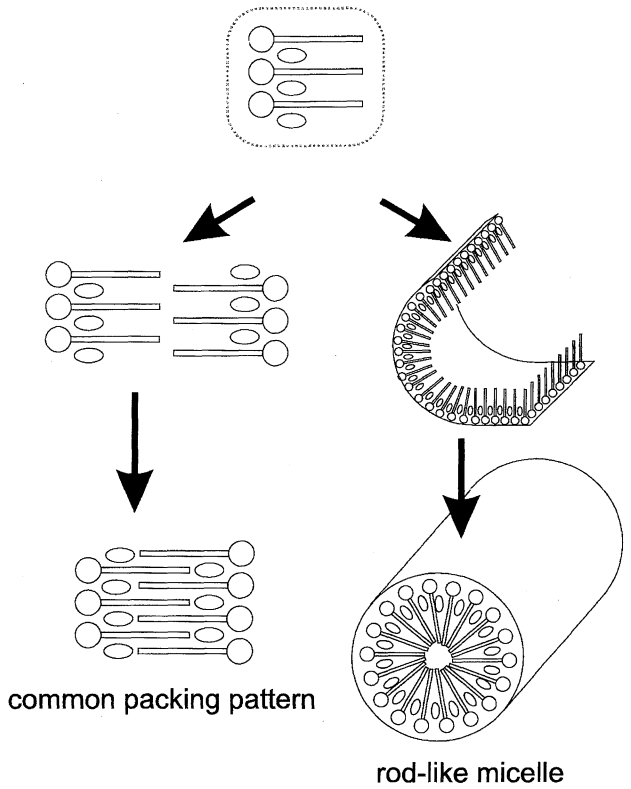

Fig. 22. Schematic drawings of single crystal formation and rod-like micelle from the elementary pattern. If a pair of elementary patterns are combined as shown in the left side, the common packing pattern in the crystals are formed. If the elementary pattern is folded to form a pipe in the right side, the rod-like micelle is made.

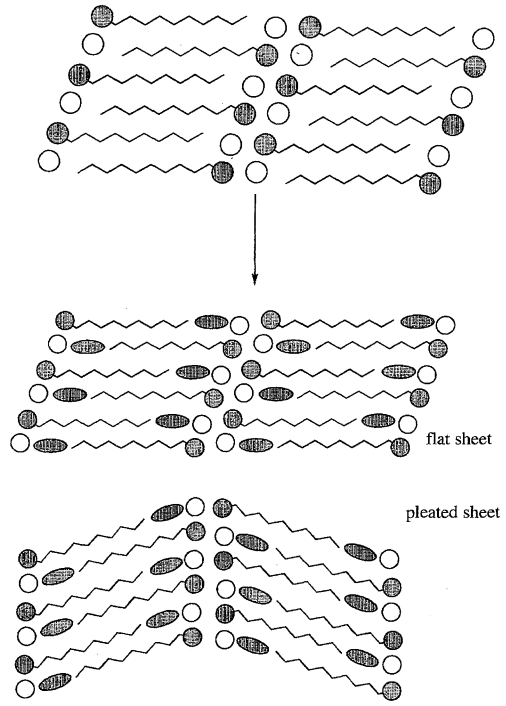

Fig. 23. Two modes of stacking of common packing patterns, flat sheet (upper) and pleated sheet (pleated).

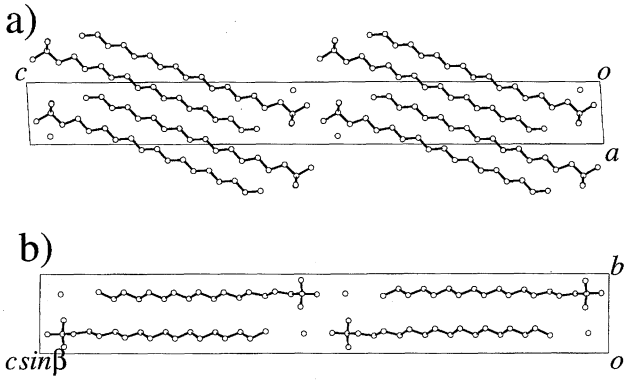

Fig. 24. Crystal structures of CTAB only viewed along the *b*; a) and *a*; b) axes. A flat sheet is formed parallel to the *ac* plane.

(7) When the above common packing pattern is piled up along the long axis of the crystal, there are two modes of stacking; the straight and bent ones, as shown in Fig. 23. In the straight mode a flat sheet is formed, but a pleated sheet is made in the bent mode.

Figure 24 shows the crystal structures of CTAB itself viewed along the *a* and *b* axes.[20] The structure also has the characteristics of the complexes described above except that it has no aromatic compound. A flat sheet composed of CTAs and the bromide anions is formed. When CTAB makes a complex with aromatic compound, the antiparallel alkyl groups of the neighboring surfactant molecules slide in opposite directions to each other as shown in Fig. 25. A gap is made between the trimethylammonium moiety and the end of the hexadecyl group. The aromatic molecules occupy the gap. The aromatic molecule in the gap is sandwiched by the alkyl chains of the upper and lower CTA molecules. The sandwiched aromatic molecule makes a hydrogen bond with the bromide anion or the solvent water molecule if it has a hydrogen donor. However, if the aromatic molecule has no hydrogen donor, it also occupy the same position as shown in the acridine–CTAB complex. These facts suggest that the layer structure as shown in Fig. 21, 3) or 4), is a common pattern of the complexes formed between the surfactant and the aromatic compound when they are dissolved in an aqueous solution.

A Model for Formation of the Gigantic Rod-Like Micelles. The common pattern of the complex formation brought about an idea that a similar structure should be made when the aromatic compound is dissolved in an aqueous solution containing surfactant. In our previous papers,[12—14] one of the authors (H. H.) reported that elongated rod-like micelles were observed by electron microscopy when CTAB and several aromatic compounds such as *o*-iodophenol and salicylic acid were dissolved in aqueous solutions. These solutions often had high viscoelasticity, which is caused by the cobweb-like entanglement of the elongated rod like micelles. These results suggest that the common pattern of the complex formation is responsible to the formation of the rod-like micelles, since the rod-like micelles and the single crystals coexist in a transmission electron micrograph of

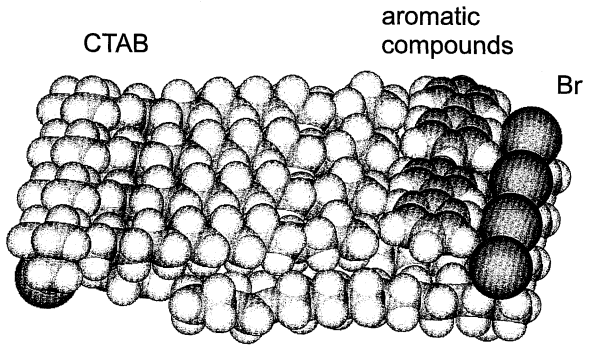

Fig. 25. Space-filling models of the complex formation between the cationic surfactant molecules and aromatic molecules.

the solution. The layer composed of CTA cation and bromide anion and aromatic compound as shown in Fig. 21 is rolled to form a tube, which is the rod-like micelle. The right side drawing in Fig. 22 shows a schematic model of the section of the rod-like micelles. The aromatic molecules connect the surfactant molecules near the surface of the rod. The complex formation between the surfactant and aromatic molecules probably strengthens the rod formation in the aqueous solution. The diameter of the rod may be more than 70 Å, since the CTA cation is about 30 Å long and about 5—10 Å may be necessary in the central part of the rod to accommodate the entangled terminal parts of the alkyl chains. Moreover, the hydrophilic exterior should be covered with water molecules. This suggests the diameter of the rod-like micelles may be estimated to be 70—80 Å. This value is shorter than the diameter of 100—120 Å suggested in our previous paper,[14] but is longer than the diameter suggested by Vinson and Talmon, 45—60 Å,[21] which was measured from cryo-TEM of hexadecyltrimethylammonium chloride–sodium salicylate–NaCl solution.

This work was partially supported by a Grant-in-Aid on Priority Areas No. 06242102 from the Ministry of Education, Science and Culture.

References

1) J. H. Fendler and E. J. Fendler, "Catalysis in Micellar and Macromolecular Systems," Academic Press, New York (1975), p. 20.
2) G. S. Stainsby and A. E. Alexsander, *Discuss. Faraday Soc.*, **11**, 150 (1951).
3) T. Nash, *J. Collid Sci.*, **13**, 134 (1958).
4) J. C. Eriksson and G. Gilberg, *Acta Chem. Scand.*, **20**, 2019 (1966).
5) J. H. Fendler and L. K. Patterson, *J. Phys. Chem.*, **75**, 3907 (1971).
6) S. J. Rehfeld, *J. Phys. Chem.*, **75**, 3905 (1971).
7) K. A. Dill, D. E. Koppel, R. S. Cantor, J. D. Dill, D. Bendedouch, and S. Chen, *Nature (London)*, **309**, 42 (1984).
8) F. M. Menger and D. W. Doll, *J. Am. Chem. Soc.*, **106**, 1109 (1984).
9) T. Tachibana, T. Yoshizumi, and K. Hori, *J. Am. Chem. Soc.*, **107**, 509 (1985); *Bull. Chem. Soc. Ipn.*, **52**, 34 (1979).
10) J.-H. Fuhrhop, P. Schnieder, J. Rosenberg, and E. Boekema, *J. Am. Chem. Soc.*, **109**, 3387 (1987).
11) J.-H. Fuhrhop, P. Schnieder, E. Boekema, and W. Helfrich, *J. Am. Chem. Soc.*, **110**, 2861 (1988).
12) Y. Sakaiguchi, T. Shikata, H. Urakami, A. Tamura, and H. Hirata, *J. Electron Microsc.*, **36**, 168 (1987).
13) Y. Sakaiguchi, T. Shikata, H. Urakami, A. Tamura, and H. Hirata, *Colloid Polym. Sci.*, **265**, 750 (1987).
14) T. Shikata, Y. Sakaiguchi, H. Uragami, A. Tamura, and H. Hirata, *J. Colloid Interface Sci.*, **119**, 291 (1987).
15) H. Hirata and Y. Sakaiguchi, *J. Colloid Interface Sci.*, **127**, 589 (1989).
16) H. Hirata, Y. Kanda, and S. Ohashi, *Colloid Polym. Sci.*, **270**, 781 (1992).
17) G. M. Sheldric, *Acta Crystallogr., Sect. A*, **A46**, 467 (1990).
18) G. M. Sheldrick, "SHELXL97. Program for the Refinement of Crystal Structures," University of Gottingen, Germany (1997).
19) "International Tables for Crystallography," Kluwer Academic Publishers, Dordrecht/ Boston/ London (1992), Vol. C.
20) A. R. Campanelli and L. Scaramuzza, *Acta Crystallogr., Sect. C (Cr. Str. Comm.)*, **C42**, 1380 (1986).
21) P. K. Vinson and Y. Talmon, *J. Colloid Interface Sci.*, **133**, 288 (1989).